JCI The Journal of Clinical Investigation

Compositional mapping of cholesteryl ester droplets in the fatty streaks of human aorta.

G M Hillman, D M Engelman

J Clin Invest. 1976;58(4):1008-1018. https://doi.org/10.1172/JCI108524.

Research Article

Frozen sections prepared from human aortic tissue containing fatty streak lesions were examined on a thermally controlled stage with a polarizing light microscope. Distinct birefringent droplets, 0.5-5 mum in diameter, were observed, many apparently aggregated into clusters. The clusters were about 20 X 20 mum in diameter (the approximate size of foam cells). Upon being heated, each smectic droplet exhibited a sudden change of birefringence, indicating a change of state. The transition temperatures were compared to assess compositional distributions in the tissue. We found that for 52% of the clusters the standard deviation of the cluster's droplet melting point distribution was less than half that observed in the surrounding microscopic field. If clusters were intracellular lipid inclusions, this observation indicates that the lipid composition within a foam cell is more homogeneous than that of the overall field. However, using statistical methods, we compared droplet melting populations from cluster to cluster and found significant heterogeneity. The observations can be interpreted to suggest that many foam cells modify the cholesteryl ester fatty acid composition of their accumulations be selective uptake, temporal sampling, or chemical reaction. Furthermore, the intercellular heterogeneity suggests that different cells in the lesion may have different metabolic and transport enzyme affinities or be in different states.

Compositional Mapping of Cholesteryl Ester Droplets in the Fatty Streaks of Human Aorta

GERALD M. HILLMAN and DONALD M. ENGELMAN

From the Department of Molecular Biophysics and Biochemistry, Yale University, New Haven, Connecticut 06520

ABSTRACT Frozen sections prepared from human aortic tissue containing fatty streak lesions were examined on a thermally controlled stage with a polarizing light microscope. Distinct birefringent droplets, 0.5–5 μm in diameter, were observed, many apparently aggregated into clusters. The clusters were about 20 × 20 μm in diameter (the approximate size of foam cells).

Upon being heated, each smectic droplet exhibited a sudden change of birefringence, indicating a change of state. The transition temperatures were compared to assess compositional distributions in the tissue. We found that for 52% of the clusters the standard deviation of the cluster's droplet melting point distribution was less than half that observed in the surrounding microscopic field. If clusters were intracellular lipid inclusions, this observation indicates that the lipid composition within a foam cell is more homogeneous than that of the overall field. However, using statistical methods, we compared droplet melting populations from cluster to cluster and found significant heterogeneity. The observations can be interpreted to suggest that many foam cells modify the cholesteryl ester fatty acid composition of their accumulations by selective uptake, temporal sampling, or chemical reaction. Furthermore, the intercellular heterogeneity suggests that different cells in the lesion may have different metabolic and transport enzyme affinities or be in different states.

INTRODUCTION

The process of accumulation of cholesteryl esters in the foam cell droplets of fatty streak atherosclerotic lesions is not well understood. We have devised a technique to observe lipid compositional differences at the light microscopic level in the hope that knowledge of the distribution of compositional differences in the lesion may reveal details of this process. In visible fatty streak lesions, most of the accumulated lipid is found in droplets 0.5–5 μm in diameter. We showed, in a separate paper (3), that the molecules of many of the droplets are organized into the liquid-crystalline smectic mesophase and that this phase melts in a thermotropic order-to-disorder transition near body temperature. The transition temperature of each droplet depends on its chemical composition and may be observed as a specific thermotropic change in the birefringent pattern of the droplet as seen in a polarized light microscope. In this paper we present a study designed to exploit the composition-dependent transition temperature to map droplet compositional differences in fatty streak lesions *in situ*.

Earlier compositional studies have involved gross chemical analysis of the lipid fractions from lesions. For instance, Smith and Slater extracted and analyzed the lipid from regions obtained by microdissection of raised fatty atherosclerotic plaques (4). These studies revealed compositional differences between regions rich in extracellular deposits and regions containing mainly intracellular droplets, but more refined characterizations were limited by dissection technique and quantity of material. In our approach the droplet melting behavior in frozen sections of fatty streak material was examined on the thermally controlled stage of a polarized light microscope. The spatial distribution of droplet melting temperatures revealed organizational principles not previously noted. Similarities in the composition of lipid droplets within cells and differences in the composition of droplets between cells suggests mechanisms involved in the process of lipid accumulation. Furthermore, this study suggests that there may be different stages of lipid accumulation in the lesion that can be characterized by the degree of droplet compositional

This work was part of the doctoral thesis of G. M. Hillman (1). A preliminary abstract of this work has been reported (2).

Received for publication 10 October 1975 and in revised form 28 June 1976.

variability within the lesion. Our approach permits an investigation of these issues.

To begin our investigation, the questions we have posed concern the distribution of compositional differences in the lipid droplets of fatty streak lesions at different levels of organization. The levels chosen for study were the individual droplets, the cell boundary, the lesion boundary, and the individual aorta. At each level of compartmentalization it was asked whether the composition of the droplets were relatively uniform with respect to that level and whether observed differences were real or coincidental.

METHODS

Source of material. The aortas from five individuals were obtained at autopsy. The age, sex, and cause of death for each individual are specified in Table I. No specimens were taken at autopsies performed more than 24 h after death. Immediately after removal from the body, the tissue was placed in an 0.9% NaCl solution. In two cases it was immediately removed from the saline for dissection. For the rest of the cases it was stored for no more than a few hours at 4°C and then dissected.

The dissection consisted of excising blocks of tissue from the aorta. Each block contained about 3 by 2 mm of lumenal surface and included fatty streak regions.[1] The blocks were then placed in buffer A solution.[2]

Frozen sections. Within minutes after dissection, one block from the buffer A solution was dropped into a plastic beaker of hexane in thermal equilibrium with a cold bath of dry ice and hexane. The procedure gives a very high freezing rate. Meanwhile, the remaining blocks in the buffer A solution were refrigerated at 4°C.

Sections 6 μm thick were cut out on a Harris cryostat (Damon/IEC Div., Damon Corp., Needham Heights, Mass.) while the knife and chamber were kept at -18°C. Usually three sections were picked up per slide. One was unstained. One was stained for 30 s in 0.03% toluidine blue. The other was stained for 1–2 min with Oil Red O (E. I. du Pont de Nemours & Co., Wilmington, Del.), prepared according to the procedure of Putt (5). Toluidine blue stains nuclei red and collagen blue. Thus, some cellular loci could be identified by the nuclei. Unfortunately, toluidine blue did not provide enough contrast to identify cell boundaries. Toluidine blue, a water-soluble dye, did not seem to affect the melting points of the lipid droplets. Oil Red O, which is cholesteryl ester-soluble, stained the droplets red and altered their melting temperature. Sections were mounted in glycerol (which does not affect the lipid phases) on glass slides and covered with cover slips. By the histological criteria defined elsewhere (3), each lesion examined in this study was identified both macroscopically and microscopically as a fatty streak.

A control experiment. To assess the effects of the freezing techniques, a sample was carried through the entire preparative procedure and monitored at different points by X-ray diffraction and light microscopy. The X-ray diffraction equipment and techniques we used are described elsewhere (1, 3). X-ray diffraction will reveal structural changes in the lipid or the appearance of new structures. An intima-media preparation containing fatty streak material plus a drop of buffer A was sealed in a capillary and examined by X-ray diffraction at 31°C. The sample exhibited the characteristic cholesteryl ester smectic phase pattern (3). When the sample was heated to 37°C, the intensity of the $(35\ \text{Å})^{-1}$ line diminished considerably, indicating that much of the diffracting material had melted. The sample was removed from the capillary and quick-frozen in a beaker of hexane-dry ice bath. After 1 min, the frozen tissue was removed from the beaker with cold tweezers and placed on dry ice for 45 min, simulating the time spent in the cryostat. Then it was thawed to room temperature, resealed in a thin-walled capillary along with a drop of buffer A, and re-examined by X-ray diffraction at 24.4°C. The characteristic $(35\ \text{Å})^{-1}$ low-angle Bragg reflection reappeared. However, a few faint Bragg reflections not observed before also appeared at smaller spacings, indicating that the sample may have begun to crystallize. These crystals could be brought into the smectic state by the appropriate thermal treatment (see below). A block of tissue was cut from the same aortic specimen and frozen sections were prepared from it. Most of the droplets melted between 36°C and 40°C, in good agreement with the X-ray studies done before the freezing step.

The microscope and temperature-controlled stage. A polarized light microscope with a specially-built temperature-controlled stage was used to study the heterogeneity in the phase transition temperatures of lipid deposits at the cellular level. Frozen sections were observed on a Zeiss RA microscope with a 40X achromat dry objective and 12.5 × Kpl eyepieces (Carl Zeiss, Inc., New York). Insertion of crossed Polaroid polarizers (Polaroid Corp., Cambridge, Mass.) into the optical system allowed us to study birefringent material. Birefringent sign could be determined by insertion of a quarter-wavelength plate into the system. The microscope stage consisted of a large brass block through which thermally controlled water circulated. A microscope slide was placed in a groove on the stage and covered with a brass plate that made thermal contact with the stage. The stage itself was mounted on a Lucite block that provided thermal insulation from the microscope. The specimen temperature was calibrated from the measurement of melting temperatures of compounds whose melting points were determined independently. Regulation was ±0.2°C near 37°C.

Thermal scans. Unstained, unfixed frozen sections, when first examined at room temperature under polarized light, contained a substantial amount of birefringent material. Most of the material was composed of irregularly shaped objects about the size of droplets and was distributed in

TABLE I
Catalogue of Specimens

Aorta specimen	Age	Sex	Cause of death
1	34	F	Laennec's cirrhosis
2	25	F	Suicide—poison
3	17	M	Severe hemolytic (Coombs-positive) anemia
4	26	M	Electrocution
5	20	M	Gunshot

[1] The criteria used to define fatty streak regions are presented in a separate paper (3).

[2] Buffer A: 0.155 M NaCl and 0.1 M Na_2PO_4, titrated to pH 7.4 with HCl.

the approximate locations of the clusters observed in subsequent scans. There were only a few spherulites or droplets exhibiting formée crosses in the field. If the sample was then heated until all the birefringent material melted (42–45°C) and then cooled back to room temperature, most of the birefringence would return, but this time there would be many spherulites exhibiting formée cross patterns.[3] What appeared to have happened was that droplets that crystallized during the quick-freeze step melted monotropically[4] to the isotropic liquid phase upon heating. After cooling they organized into mesophase states, and subsequent thermal scans revealed the mesophase transition temperatures of the droplets. A comparison of fields before and after the melting step revealed no change in the general distribution of birefringent material in the tissue, except that crystals were replaced by droplets. Although it is not possible to exclude it absolutely, it appeared that the crystals did not, in general, merge to give larger droplets; there was no rearrangement of cluster boundaries. Droplets observed in freshly autopsied material that had never been frozen were shown by X-ray diffraction to be in the smectic state and not in a crystalline state (3). Thus, it seems reasonable to suppose that heating scans subsequent to the first one reveal phase behavior more closely resembling the state in vivo than first heating scans after freezing. Hence, statistical analyses were performed on subsequent heating scans rather than initial ones.

Thermal scans were usually started at about 25°C. The section was mounted on a microscope slide under a coverslip with glycerol. Thus, the specimen was not directly exposed to the atmosphere and oxidative degradation was kept at a minimum. The sample was photographed, heated by an increment of 1.5–2.0°C, and photographed again. It took less than a minute to heat the sample 2°C. Nevertheless, at least 5 min was allowed for the system to come to equilibrium after each heating increment. Photographs as a function of time revealed no further changes upon prolonged equilibration. The procedure was repeated until all the droplets melted and then the system was cooled back to the initial temperature. Cooling took about 30 min. Afterwards, the sample was photographed to demonstrate the reversibility of the phase transitions. A scan takes about 2 h to perform. The last scan was completed within 15 h of autopsy.

Data analysis. Pictures of the scan were taken on black-and-white film. Three types of birefringent patterns emerged: sharp bright spots, formée cross patterns (which we call droplets), and diffuse, amorphous birefringence (see Fig. 2). Patterns exhibiting the formée cross have in general proved to be positively birefringent (7), although not all droplets in the present study were examined with respect to sign. This information, when combined with X-ray measurements, has demonstrated a smectic organization. However, the possible existence of droplets in the nematic phase cannot be absolutely excluded, since diffraction studies are insensitive to the presence of such structures in tissues (3). We interpret the droplets (having the formée cross) as being in the smectic state, although the arguments of this paper do not depend on the correctness of such an interpretation. The sharp spots probably arose from small smectic droplets and the amorphous material was unidentifiable but possibly material organized in the cholesteric phase (3).

The birefringent droplets were often observed to be aggregated. If three or more spots or droplets were aggregated into an area smaller than 20 × 20 μm (the size of a foam cell), the aggregation was called a cluster. In some cases there were huge birefringent accumulations that consisted of many small droplets and spots or one to several large droplets (10–15 μm in diameter) or just a large continuous irregularly shaped birefringent mass, 20–30 μm across. Such accumulations were classified as lipid pools. Finally, spots or droplets that did not appear in a clearly definable cluster were called isolated spots or droplets.

We interpreted both the loss of birefringent activity of a spot and the deformation of the formée cross in a droplet as arising from the melt of either object from the smectic to a less ordered phase. Since the diffuse, amorphous birefringent material probably was not in the smectic state, the loss of its birefringence corresponds to a different phase transition. Hence, amorphous component melting behavior was deleted from statistical treatments. The size and smectic melting point of every component was recorded and this information was kept for each aggregation in the field. The melting temperature of a cluster was defined as the average melting temperature of its components.

Clusters might correspond to intracellular deposits. Although the definition of a cluster is somewhat qualitative,

TABLE II

An Example of Raw Data from a Typical Scan (from Aorta 5, Lesion 1, Field 2)

Aggregation	T_m	Droplet diameter	Spot diameter	Aggregation size
	°C	μm	μm	μm × μm
Cluster A	30.5	3.9		
	32.5	1.4		25 × 11
	34.7	0.9, 1.4, 2.1, 3.6		
	35.4	1.6, 2.1		
	36.5	1.5, 2.5, 2.9		
Isolated components				
1	40.4	2.9		
2	30.5	1.4		
4	28.5	2.9		
5	28.5	2.5		
6	32.5	2.5		
7	36.5	1.4		
8	32.5	1.4		
9	28.5	0.7		
10	26.5	2.1		
11	30.5		0.7	
12	26.5		1.4	

Summary of results.

	n	T_m°C	σ
11 droplets in the cluster	11	34.7	1.8
11 isolated droplets and spots in the field	11	31.0	4.3
22 total droplets and spots in the field	22	32.9	3.7

Human atherosclerotic tissue was examined by polarized light microscopy in approximately 2°C intervals in a heating scan. At each interval endpoint the tissue was allowed to come to thermal equilibrium and then it was photographed. If a droplet or spot was visible at, for example, 30.5°C but deformed or lost its birefringence at 32.5°C, we assign it a melting temperature (T_m) of 32.5°C and record its size in the appropriate column for droplets or spots. The initial temperature for this scan was 24.5°C. In the summary, the average melting temperature and standard deviation of the components within the cluster, outside of the cluster, and of the field are given.

[3] A few droplets exhibiting formée cross patterns were observed to form from birefringent material during heating. Presumably this was due to the enantiotropic melting of a few crystals to the smectic mesophase state.

[4] See ref. 6 for a discussion of monotropism.

in most cases, cluster boundaries were quite obvious (Fig. 2). The lipid pools consisting of many spots and droplets might be either extracellular deposits or the intracellular deposits of several aggregated cells. The melting points of the components of such aggregations were included for overall microscopic field analysis; however, because only a few of these aggregations were observed, they were not analyzed further. Lipid pools consisting of huge (>10 μm) droplets and spots or the large, irregular-shaped continuous lipid pools could be extracellular deposits; alternatively, they could be artifacts arising from knife smears or from the freeze-melt preparation procedure. These lipid pools were deleted from our statistical treatments. Lipid pools were predominant in some fields. Many fields had none. The birefringent areas not excluded on the basis of the above criteria were used in the statistical analyses.

The compositional variability within clusters was analyzed by comparing the melting points of the component droplets and spots of one cluster with those of all the droplets and spots in the photographic field surrounding the cluster. Statistically the comparison was made between the standard deviation from the mean melting temperature of the droplets and spots in the field. If the spread of the cluster's component melting point distribution curve was less than that of the field, the cluster component melting distribution was said to be more closely grouped than that of the field.

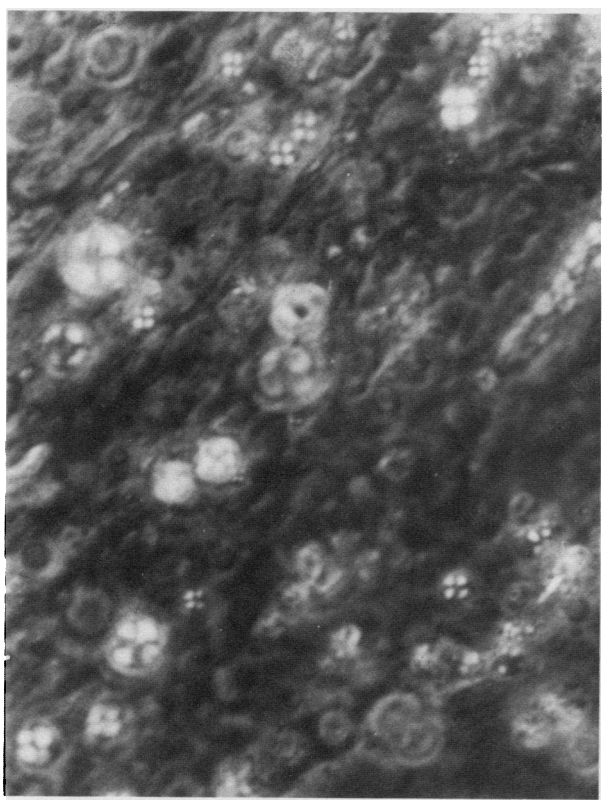

FIGURE 1 Clusters and their morphological location. Human aortic material was frozen-sectioned and observed under quarter-wave polarizing conditions. Under such illumination, both birefringent material and the surrounding intimal tissue may be observed. This photomicrograph, taken at 25°C, shows many birefringent droplets exhibiting formée crosses. Note the cluster of formée-crossed droplets in the upper right corner. Running diagonally, the striations of the media begin in the upper left corner. The lumen is off the picture but would be in the lower right corner.

FIGURE 2 Cluster boundaries. This is the same section as shown in Fig. 1 except that it is under crossed-polarizing illumination. Under these conditions only birefringent material is visible, but there is better sensitivity. Many of the formée-crossed droplets pictured in Fig. 1 have been overexposed here and appear as bright spots. Boundaries have been sketched around droplets showing their apparent clustering. Notice the amorphous material in the large cluster centered at the bottom. This may be material organized in the cholesteric state. Many of the large spots do not exhibit formée crosses simply because they are out of focus. In these thick sections, depth-of-field may be problematic. The bar in the upper left corner delineates 10 μm.

Table II contains the data obtained from a temperature scan. The field contained only one cluster, which consisted of 11 droplets. It was surrounded by 11 isolated droplets and spots. Photographs were taken at approximately 2°C intervals. When a droplet is reported to have melted at 32.5°C, it means that its birefringent pattern disappeared within the range from 30.5° to 32.5°C. In this scan an intermediate point was observed at 35.4°C, giving two approximately 1° intervals. The droplets are observed to melt sharply, even within the 1° intervals. Table II (bottom) shows the average melting temperature and the standard deviation for droplets and spots in the cluster only, isolated from the cluster, and in the entire field including the cluster. In this study the standard deviation of the cluster melting components was compared to that of the entire field. In most fields the components of any given cluster constituted only a small percentage of the total droplet and spot popu-

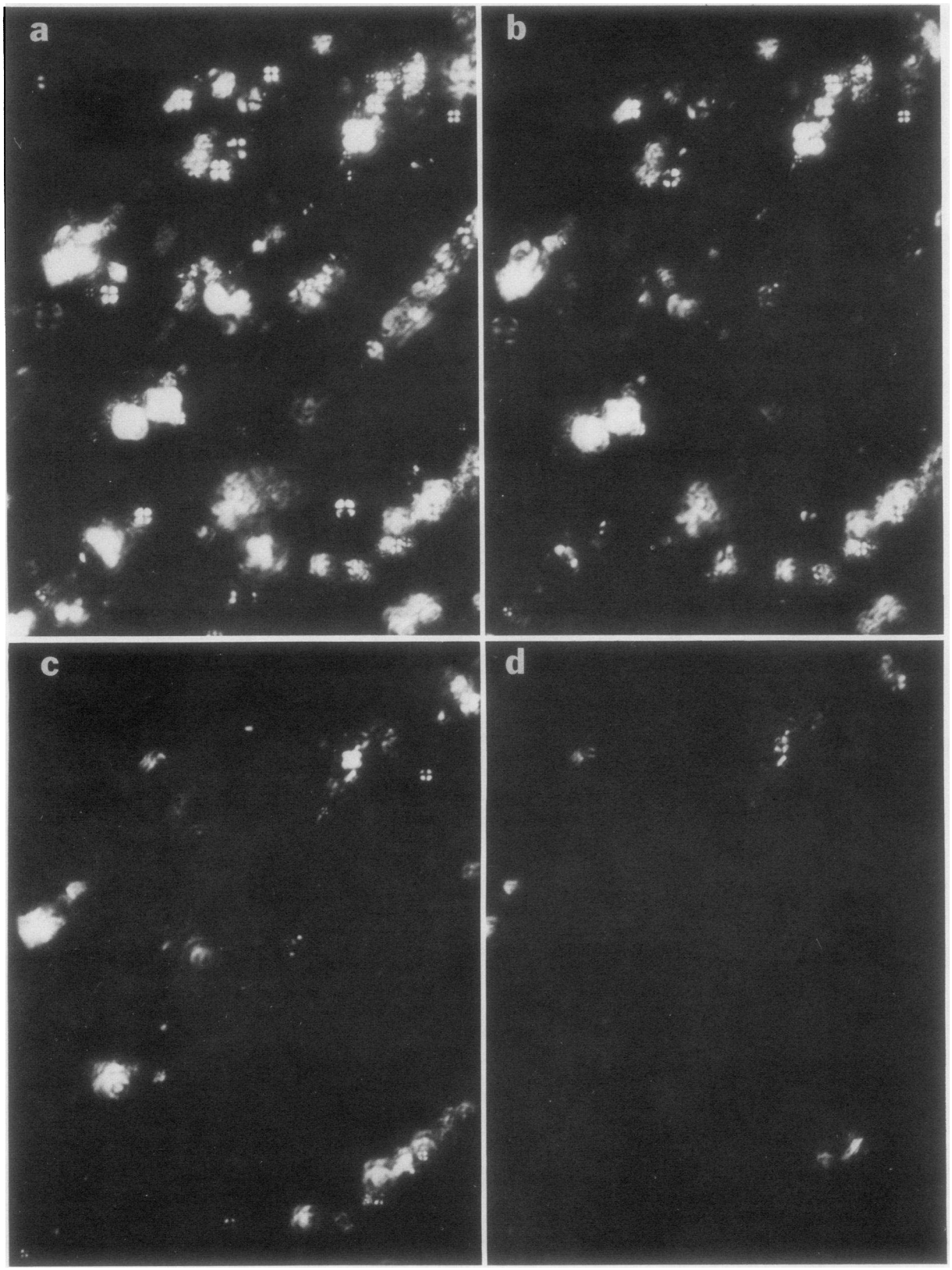
a
b
c
d

lation in the field. Although the melting points of the droplets and spots are not normally distributed, the standard deviation is still a rough measure of the spread of the melting point distribution. The ratio of the standard deviation of the component melting distribution of the field to the standard deviation of the cluster component melting distribution was $3.7/1.8 = 2.1$, indicating the close grouping of the cluster component melting points.

The compositional variability among clusters was evaluated by determining the probability of significant difference between two population distributions. There is no a priori reason to assume a normal distribution for the melting points of the droplets and spots. In fact, the overall distribution of melting points for the 599 droplets and spots was skewed, leptokurtotic, and bimodal. Hence, the assumption of normality for parametric testing was not fulfilled by our data and we had to use nonparametric (distribution-free) statistical tests to examine population differences. Our sample populations were often small and unequal. Therefore, we examined population differences using the Mann-Whitney U test, a powerful nonparametric test applicable to unequal sample sizes and to sample populations as small as three (8).

64 clusters, composed of 599 droplets and spots, were studied. The clusters examined were from 5 aortas, 7 lesions, and 12 fields.

RESULTS

Frozen sections were prepared from the fatty streak lesions of five aortas and examined with a polarized light microscope. One section appears in Fig. 1, illuminated with polarized light and a quarter-wavelength plate. The lumen, the intima, and a small part of the media are visible in this photograph. Several birefringent droplets in the tissue displaying formée crosses also appear. When the quarter-wave plate is removed, the background tissue becomes completely dark and only birefringent material is visible (Fig. 2). The sharp spots and the droplets exhibiting the formée cross configuration are accumulated cholesteryl esters organized in the smectic state. The cluster boundaries for this section have been sketched in Fig. 2.

Photomicrographs from the thermal scan of this section are shown in Fig. 3. As the temperature was raised, the crosses deformed and disappeared, and the birefringence became diffuse. This was probably due to a phase transition from the smectic to the cholesteric phase. However, bright-field illumination revealed that the droplets and spots remained intact. As the material was heated further, the birefringent areas vanished (Fig. 3*b*, *c*, *d*). The esters had melted into the isotropic liquid phase, which is not birefringent. Again, bright-field illumination showed that the droplets remained intact. On cooling, the droplets regained their original birefringent patterns, demonstrating that the phase transitions were reversible (compare Fig. 2, taken at 25°C after the scan, with Fig. 3*a*, taken at 27°C before the scan). Although the scan is shown at 4°C intervals, the sections were photographed and analyzed at 2° intervals.

The accumulated lipid droplets appeared to be aggregated into clusters about the size of foam cells. Careful examination of the melting behavior of the field revealed that, for many clusters, the constituent droplets all melted sharply and exhibited similar phase transition temperatures. This gave many clusters a well-defined characteristic transition temperature. However, in the same microscopic field, the characteristic transition temperature varied from cluster to cluster by several degrees.

To substantiate these observations statistically, the photomicrographs clearly required the evolution of a systematic method. The first task was to abstract the information contained in the scanning photomicrographs and to translate it into a usable form for data reduction. Birefringent material was classified by its distribution (clusters, lipid pools, or isolated droplets and spots), and then the clusters and pools were subdivided into their component droplets and spots. The melting characteristics of each of the components were then recorded. The data were used to analyze the distribution of droplet melting points within clusters and to compare droplet melting point distributions from cluster to cluster.

First, we examined whether or not the melting point distribution of the droplets and spots in a cluster was more closely grouped than the melting point distribution of all the droplets and spots in the field (area observed in a scan). The standard deviation of the melting point distribution for the droplets in each cluster was compared with the standard deviation of the melting point distribution for the droplets and spots in the entire

FIGURE 3 Thermal scan of human early fatty streak material. This scan was actually performed at 2°C intervals, but for brevity photographs of every other point in the scan are shown. (*a*) 27°C; (*b*) 31°C: notice the disappearance of the large cluster in the middle on the right edge of the photomicrograph. The cluster has melted. Also, note the two adjacent large droplets in the left lower portion. (*c*) 35°C: One of these droplets melts. A cluster remains in the bottom right. (*d*) 39°C: The other large droplet melts and the cluster in the lower right melts. Only a few droplets remain unmelted. After the heating scan, the sample was cooled to 25°C and the photomicrograph of Fig. 2 was obtained. Comparison of Fig. 2 with Fig. 3*a*, the initial point of the scan, shows that the droplets and spots returned, thus demonstrating the reversibility of the phase transition. Notice the return of additional droplets not seen at 27°C. Presumably these new droplets melt between 25°C and 27°C.

TABLE III

Intracluster Homogeneity: The Standard Deviation of a Cluster is Compared with That of Its Surrounding Field

Cluster*	Cluster parameters			Field parameters			$\left(\frac{\sigma_{field}}{\sigma_{cluster}}\right)$
	n‡	T_m§	$\sigma_{cluster}$‖	n¶	T_m**	σ_{field}‡‡	
1.1.1							
A	5	33.1	2.9				1.0
B	6	36.0	1.6				1.9
C	6	36.4	2.9	42	37.5	3.0	1.0
D	4	37.3	1.5				2.0
E	3	38.7	1.1				2.7
F	6	38.8	0.4				7.5
G	8	40.9	0.5				6.0
1.1.2							
A	3	39.5	0				∞
B	3	39.5	0				∞
C	4	39.5	0	39	41.0	1.9	∞
D	6	40.5	1.1				1.7
E	6	41.2	0.8				2.4
F	3	41.5	2.0				0.9
G	3	41.5	2.0				0.9
H	4	41.5	2.3				0.8
I	5	43.5	0				∞
1.1.3							
A	4	34.0	0				∞
B	5	34.4	0.9				3.1
C	7	36.6	1.2	71	37.8	2.8	2.3
D	3	36.7	3.1				0.9
E	8	37.1	3.1				1.6
F	5	37.3	2.2				1.3
G	6	37.8	1.6				1.8
H	17	41.0	0.9				3.1
2.1.3							
A	6	31.5	0	38	34.8	3.0	∞
B	8	35.3	0.94				3.2
3.1.1							
A	4	36.0	2.8				0.9
B	4	36.5	3.0				0.8
C	5	36.6	3.4				0.7
D	3	36.7	1.1	60	37.2	2.4	2.2
E	7	37.3	3.1				0.8
F	5	37.4	2.4				1.0
G	7	37.9	1.9				1.3
H	3	38.7	1.1				2.2
I	5	38.8	3.9				0.6
4.1.2							
A	4	22.0	0				∞
B	7	22.0	0	49	25.6	6.1	∞
C	5	22.9	1.5				4.0
D	3	23.7	1.4				4.4
E	4	24.5	0				∞
4.2.1							
A	5	25.2	0.4				15.7
B	6	37.1	3.9	29	32.3	6.3	1.6
C	3	39.6	2.7				2.3
4.2.2							
A	9	33.8	4.9	22	31.7	5.0	1.0
5.1.1							
A	8	30.7	2.5				1.6
B	5	31.8	1.0	86	32.1	3.9	3.9
C	12	32.3	3.4				1.1
D	9	34.0	4.6				0.8
E	6	37.8	1.7				2.3
5.1.2							
A	11	34.7	1.8	22	32.9	3.7	2.1
5.2.1							
A	5	26.6	1.4				2.7
B	6	28.7	1.3				2.9
C	6	29.2	0	99	31.9	3.8	∞
D	8	29.7	1.5				2.5
E	6	31.3	3.2				1.2
F	8	31.8	3.3				1.1
G	11	33.1	2.8				1.4
H	8	34.0	2.9				1.3
I	10	35.9	4.7				0.8
5.2.2							
A	11	29.0	0				∞
B	6	31.4	2.8	42	31.4	3.5	1.2
C	7	32.5	3.7				0.9
D	4	33.2	3.4				1.0
E	6	35.5	0				∞

* "2.1.3" designates aorta 2, lesion 1, field 3. Letters refer to clusters.
‡ Number of droplets and spots in the cluster.
§ Average melting temperature of the droplets and spots in the cluster.
‖ Standard deviation of the droplet and spot melting temperatures in the cluster.
¶ Number of droplets and spots in the field.
** Average melting temperature.
‡‡ Standard deviation of the droplet and spot melting temperatures in the field.

field, and the results are shown in Table III. In 52% of the cases $\sigma_{field} > 2\sigma_{cluster}$, indicating that the majority of clusters were considerably more closely grouped with respect to their component melting distributions than the overall field.

Another way to demonstrate this relative homogeneity is to test whether the components of each cluster may be random samples of a common imaginary parent population. Thus, a null hypothesis test was used to investigate intercluster heterogeneity. The melting point distribution of every possible pair of clusters in a field were compared by the Mann-Whitney U test of non-parametric statistics (8). The results for two characteristic fields appear in Table IV*a* and *b*. The scores have been converted to the probability that the two cluster populations are random samples from an imaginary parent population. If there is only a 5% probability that the two clusters were sampled from the same imaginary parent population, then the two clusters are said to differ significantly at the 5% level of confidence. For instance, in Table IV*a* there is a 5% probability that cluster A and cluster B are the same. The ratio of the number of significantly different pairs (that is, within the 5% level of confidence) to the

TABLE IV

Examples of Pairwise Inter-cluster Comparisons

Cluster	n	T_m	σ	Probabilities B	C	D	E	F	G	H	I
		°C					%				
(*a*) From aorta 1, lesion 1, field 3.											
A	4	34.0	0	5.0	0.8	15.9	1.7	5.0	1.0	0.2	
B	5	34.4	0.9		1.1	23.4	1.9	4.8	1.0	0.1	
C	7	36.7	1.2			73.4	56.2	51.6	19.7	0.0	
D	3	36.7	3.1				41.2	65.3	51.6	1.7	
E	8	37.1	1.8					77.2	47.8	0.9	
F	5	37.3	2.2						64.6	0.2	
G	6	37.8	1.6							0.1	
H	17	41.0	0.9								
(*b*) From aorta 3, lesion 1, field 1.											
A	4	36.0	2.8	66.7	66.7	47.8	14.9	14.2	21.9	21.5	27.1
B	4	36.5	3.0		74.9	85.7	63.8	46.5	39.5	37.9	27.1
C	5	36.6	3.4			51.6	88.9	85.7	88.9	79.5	51.6
D	3	36.7	1.1				91.2	14.2	56.9	12.6	18.0
E	7	37.3	3.1					92.8	56.9	49.7	37.3
F	5	37.4	2.4						68.2	45.3	34.7
G	7	37.9	1.9							56.9	22.2
H	3	38.7	1.1								37.3
I	5	38.8	3.9								

The cluster name, the number of droplets in the cluster (n), their average melting temperature (T_m), and the standard deviation of the component melting point distribution for each cluster in the field (σ) is given on the left. The probability that a pair of clusters have the same component melting point distribution has been determined by the Mann–Whitney U test. This probability for each pair of clusters is given as a percentage on the right. The cluster designations are simply for the designation of specific clusters and do not refer to cluster types.

total number of pairs of clusters in the field is the heterogeneity ratio and gives an index of the amount of intercluster heterogeneity in the field. These ratios are given in Table V. We found that the heterogeneity ratios ranged from 16/28 to 0/36. The average heterogeneity ratio was 0.34.

Although the data is not extensive, it is possible to make general comparisons of the transition behavior of different aortas. We sampled the droplet and spot melting point distribution of an aorta by combining the data from all the fields we investigated in the aorta. Clearly the sampling was problematic, since a distinct minority of the lesions in the artery were considered. With this qualification, aorta distributions were compared pairwise by the Mann-Whitney U test and the results are shown in Table VI.

DISCUSSION

The lipid droplets in human fatty streak lesions, when heated, underwent thermotropic phase transitions that we observed with a polarized light microscope. Droplets isolated from the tissue and analyzed chemically were found to be almost pure cholesteryl esters (3), as originally reported by Lang and Insull (9). This suggested that the known mesophase behavior of synthetic cholesteryl esters (6, 10, 11) may account for the observed phenomena. Coordinated use of X-ray diffraction (3) and polarized light microscopy (7) allowed us to argue that the strongly birefringent droplets under the microscope are *in situ* lipid droplets in the smectic state. In the 2°C intervals of the heating scan, some droplets first melted from the smectic phase to a state that exhibited a diffuse birefringent pattern and then at higher temperatures melted to a nonbirefringent state, while other droplets simply appeared to melt directly into the nonbirefringent state. On the basis of known cholesteryl ester behavior (6, 10, 11), we interpreted the diffuse birefringent pattern as arising from droplets organized in the cholesteric state and the nonbirefringent pattern as arising from droplets organized in the isotropic liquid phase. The droplets that appeared to melt directly from the smectic state to the liquid state presumably had a cholesteric temperature range too narrow to be observed with a 2°C scanning interval.

TABLE V

Summary of the Intercluster Heterogeneity Mann–Whitney U Tests

Scan number*	Heterogeneity ratio‡
1.1.1	10/21
1.1.2	6/36
1.1.3	16/28
2.1.3	1/1
3.1.1	0/36
4.1.2	1/10
4.2.1	2/3
5.1.1	3/10
5.2.1	18/36
5.2.2	4/10

The component melting point distribution for one cluster in a field was compared to that of another cluster in the field by the Mann–Whitney U Test. The test yields the probability that the two populations are random samples of a larger, imaginary parent population. If the probability is 5% or less, the pair is considered significantly different. All possible pairs of clusters are compared in each field. The heterogeneity ratio is given by the number of pairs significantly different divided by the total number of pairs in the field. For instance, scan 1.1.3 (see Table IV*a*) has 16 pairs of clusters whose droplet melting point populations differ significantly at the 5% level of confidence out of a possible 28 pairs of clusters. Its heterogeneity ratio is 16/28.

* (aorta). (lesion). (field).

‡ (Number of pairs significantly different at 5% level)/(total number of pairs tested in the field).

Mapping compositional differences. There is much evidence that the droplet melting temperature reflects the cholesteryl ester fatty acid distribution of the droplets. First, it was shown that the droplets are almost entirely cholesteryl esters (9). Second, the sharpness of the melt (< 1°C) demonstrates that the droplets are composed of a homogeneous solution capable of a highly cooperative transition. Such a solution would have to be relatively free from impurities that would distort cholesteryl ester mesophases. Krzewski and Porter (12), studying the binary phase diagrams of three pairs of cholesteryl esters, found that cholesteryl ester mixtures form homogeneous solutions. Third, they also found in binary systems that mesophase transition temperatures are a linear function of molar composition (12). This suggests that the melting temperature of a multicomponent system would also reflect an averaging of the constituent properties. The smectic transition temperature ranges from 33°C to 39°C for a binary system of cholesteryl linoleate and cholesteryl oleate, the major esters found in atherosclerotic lesions. Addition of other esters could readily extend this range to the 20°C–45°C melting range observed for smectic droplets in the tissue.

Although the melting temperature alone may not reveal the chemical composition of the droplet, differences in droplet melting temperatures reveal the presence of compositional differences. Thus, we were able to use the temperature of the transition from the smectic phase to obtain compositional distribution maps of the tissue.

Compositional differences at the cellular level. When visible early fatty streak material was subjected to embedding, sectioning, and staining treatments (which may affect lipid structure), it was possible to differentiate between intracellular and extracellular deposits. Such studies showed that most of the lipid of the visible fatty streak was intracellular (13), a finding confirmed in electron microscope studies (14). We attempted and failed to stain cell boundaries on parallel sections by localization of the plasma membrane enzyme 5′-nucleotidase (15). Nevertheless, the droplets in a cluster are about the size of foam cells. Furthermore, the defined clusters seen must arise from some constraining force that localizes them in small areas of the tissue. The obvious existence of constrained regions and the characterizations done by others using light and electron microscopy led us tentatively to conclude for purposes of interpretation that the clusters are intracellular deposits.

Droplets that appeared to be in foam cells also appeared to have similar melting temperatures. For 52% of the clusters, the standard deviation of the cluster component melting distribution was less than half the standard deviation of the overall field component distribution. This implies that in the majority of the foam

TABLE VI

Pairwise Comparisons between Aortas

Aorta	*n**	T_m‡	σ§	Probabilities‖ 5	2	3	1
		°C			%		
4	99	29.0	6.7	0.01	0.00	0.00	0.00
5	132	31.7	3.3		0.01	0.00	0.00
2	52	34.3	2.7			0.00	0.00
3	77	37.3	2.4				0.03
1	146	38.8	2.9				

* Number of droplets and spots from the combined lesion populations observed in the aorta. Lesion populations arose from the combined droplet and spot populations of the fields observed in each lesion.

‡ Average droplet and spot melting temperature in the aorta.

§ Standard deviation of the droplet and spot melting temperatures in the aorta.

‖ Aorta populations were compared by the Mann–Whitney U test and the resultant probability that the droplet and spot melting point distributions in two aortas were the same is shown here.

cells (clusters) the chemical composition of their droplets was more homogeneous than the composition of the droplets in the surrounding field. Thus individual foam cells appear to regulate the cholesteryl ester fatty acid composition of their lipid inclusions, either through selective transport or modification.

While the droplet population within a foam cell appeared to be relatively homogeneous, the average melting temperature from foam cell to foam cell often differed by several degrees. To test whether these differences were significant, cluster droplet populations were compared by tests of the null hypothesis. Because no assumptions could be made concerning the melting point distribution of the droplets in the tissue, intercluster heterogeneity was examined by means of nonparametric (distribution-free) statistical methods. Because sample sizes were often small and unequal, the Mann-Whitney U test (8) was used to compare pairs of cluster component melting distributions.

At the 5% level of confidence, 32% of the possible cluster pairs were significantly different for the entire study. One would not necessarily expect 100% heterogeneity from these studies. That there was heterogeneity in every field but one and that in one field it ranged up as high at 57% is significant. This heterogeneity, if intercellular, implies that cells modify their cholesteryl ester fatty acid composition differently. This would argue against a monoclonal origin of foam cells. Alternatively, it may imply that the cells are in different stages of an ester modification process.

The question of intracluster homogeneity and intercluster heterogeneity are related. Since the melting point distribution within most clusters was narrower than the melting point distribution of the surrounding droplets, and since the surrounding droplets included many droplets that constituted other clusters, it is likely that cluster distributions should differ. Our results show that the heterogeneity of cluster behavior is greater than expected from random segregation. If clusters are intracellular deposits, the mechanism producing the heterogeneity may be one or a combination of three possibilities: (*a*) The cell regulates its droplet composition by the selective uptake of serum lipoproteins of a restricted range of fatty acid spectra. (*b*) The cell modifies the composition of the droplets through intracellular catabolism and anabolism of cholesteryl esters. (*c*) The cell incorporates cholesteryl esters during a restricted time period, thus sampling compositional fluctuations in the serum. Others have suggested the existence of cellular mechanisms to modify the cholesteryl ester fatty acid distribution in fatty streak lesions (4, 9, 13). The suggestions were based on the fact that the cholesteryl oleate: cholesteryl linoleate ratio was higher in lipid extracted from fatty streak lesions than in lipids extracted from serum lipoproteins. Postulates for these mechanisms must now explain the existence of compositional heterogeneity as well.

Preliminary examination of droplet melting populations within lesions has revealed the existence of both heterogeneous and homogeneous regions. Furthermore, when droplet melting distributions were compared between lesions of the same aorta, some were found to be heterogeneous. Interlesion heterogeneity suggests that there may be different kinds of lesions or that the lesions may be in different stages of development. Intralesion heterogeneity may arise from the fusion of two different types of lesions or may reflect a lesion in transition from one state to another. Finally, when aorta droplet melting distributions were compared, all aortas in the study differed significantly at the 3% level of confidence. Perhaps this arose from differences in dietary habits and metabolic activities between individuals. Aorta heterogeneity is supported by the X-ray diffraction studies (3). The wide range of average melting temperatures observed for fatty streak materials from different aortas reflects the heterogeneity observed among aorta droplet populations. The present study is too restricted to attempt correlations with epidemiological parameters known to be significant in atherogenesis. A possible future course would be to broaden the study to discover whether, for example, the distribution of transition temperatures in an artery can be related to such parameters.

ACKNOWLEDGMENTS

We are indebted to Dr. L. L. Waters of the Yale Medical School for his useful advice and criticism of this work.

This study was supported by grant HL 14111 from the National Heart and Lung Institute.

REFERENCES

1. Hillman, G. M. 1975. Thermotropic states of lipid deposits in human atherosclerotic fatty streak lesions. Ph.D. Thesis. Yale University, New Haven, Conn. (Available from University Microfilms International, Ann Arbor, Mich.).
2. Hillman, G. M., and D. M. Engelman. 1975. Phase transitions in atherosclerotic fatty streak lesions. *Fed. Proc.* **34**: 236. (Abstr.)
3. Engelman, D. M., and G. M. Hillman. 1976. Molecular organization of the cholesteryl ester droplets in fatty streaks of human aorta. *J. Clin. Invest.* **58**: 997–1007.
4. Smith, E. B., and R. S. Slater. 1972. The microdissection of large atherosclerotic plaques to give morphologically and topographically defined fractions for analysis. I. The lipids in the isolated fractions. *Atherosclerosis.* **15**: 37–56.
5. Putt, F. A. 1956. Flaming red as a dye for the demonstration of lipids. *Lab. Invest.* **5**: 377–379.
6. Small, D. M. 1970. The physical state of lipids of biological importance: cholesteryl esters, cholesterol, tryglyceride. *In* Surface Chemistry of Biological Systems.

M. Blank, editor. Plenum Publishing Corporation, New York. 55–82.
7. Hata, Y., J. Hower, and W. Insull, Jr. 1974. Cholesteryl ester-rich inclusions from human aortic fatty streak and fibrous plaque lesions of atherosclerosis. I. Crystalline properties, size and internal structure. *Am. J. Pathol.* **75**: 423–456.
8. Siegel, S. 1956. Nonparametric Statistics for the Behavioral Sciences. McGraw-Hill Book Company, N. Y. 312 pp.
9. Lang, P. D., and W. Insull, Jr. 1970. Lipid droplets in atherosclerotic fatty streaks of human aorta. *J. Clin. Invest.* **49**: 1479–1488.
10. Gray, G. W. 1956. The mesomorphic behaviour of the fatty esters of cholesterol. *J. Chem. Soc. (Lond.).* **3**: 3733–3739.
11. Davis, G. J., R. S. Porter, J. W. Steiner, and D. M. Small. 1970. Thermal transitions of cholesteryl esters of C_{18} aliphatic acids. *Mol. Cryst. Liq. Cryst.* **10**: 331–336.
12. Krzewki, R. J., and R. S. Porter. 1973. Phase studies on binary systems of cholesteryl esters: Three C_{18} ester pairs. *Mol. Cryst. Liq. Cryst.* **21**: 99–124.
13. Smith, E. B., P. H. Evans, and M. D. Downham. 1967. Lipid in the aortic intima. The correlation of morphological and chemical characteristics. *J. Atheroscler. Res.* **7**: 171–186.
14. Geer, J. C. 1965. Fine structure of human aortic intimal thickening and fatty streaks. *Lab. Invest.* **14**: 1764–1783.
15. Chayen, J., L. Bitensky, and R. G. Butcher. 1973. Practical Histochemistry. John Wiley & Sons, Inc., New York. 271 pp.